Research Article ISSN Online: 2783-4859 Computational Mathematics and Computer Modeling with Applications

Received 26 February 2025
Accepted 31 July 2025

DOI: 10.48308/CMCMA.4.1.21
AMS Subject Classification: 92C40; 92D30; 65L10

A mathematical modeling evaluating the role of booster vaccine and Quarantine strategy as interventions for cholera control

M.K. Kolawole[a] and S.R. Adebayo[a]

Cholera remains a global health challenge, especially in regions with inadequate water and healthy sanitation scheme . This research investigates the effectiveness of booster vaccination and quarantine strategies in controlling cholera outbreaks using a mathematical model that incorporates key epidemiological factors such as infection rates, recovery rates and waning immunity. The model also integrates booster vaccination to prolong immunity and quarantine measures to reduce contact between susceptible and infected individuals. Qualitative analysis of the model in lieu of sensitivity testing, demonstrates that the combined use of booster vaccination and quarantine significantly lower the basic reproduction number (R_0), effectively for controlling cholera transmission. The Laplace Adomian Decomposition Method (LADM) was used to solve the system and numerical simulation which confirm that booster vaccination enhances long-term immunity, while quarantine measures reduce transmission by limiting contact between infected and susceptible populations. Results provide valuable a valuable insights that can guide policymakers in developing more effective cholera prevention strategies to reduce disease incidence and mortality.

Keywords: Cholera; Booster vaccination; Quarantine strategies; Mathematical modeling; LADM.

1. Introduction

Cholera is a waterborne disease caused by the bacterium *vibrio cholerae*, primarily transmitted through the consumption of contaminated food and water. This pathogen thrives in aquatic environments, especially in regions lacking adequate sanitation and clean water supply. The transmission risk escalates considerably during natural disasters such as floods and hurricanes, which disrupt water and sanitation systems, creating conditions that leads to cholera outbreaks [4, 11]. Whenever unhealthy food or water is ingested, vibrio cholerae colonizes the small intestine, producing cholera toxin that leads to severe dehydration due to rapid fluid loss which often result to death if untreated [6]. The rapid spread of cholera in overcrowded and unsanitary conditions can lead to large-scale epidemics, particularly in vulnerable populations [19].

The impact of cholera extends far beyond immediate health risks, especially in low-resource settings. High mortality rates are often observed among young children, the elderly, and those with compromised immune systems [20, 3]. The urgent need for medical intervention during outbreaks frequently overwhelms local healthcare systems [15]. To a measurable extent, mathematical problem is defined by integral operator which play a crucial role in various disciplines [1]. Moreover, cholera outbreaks disrupt daily life and economic productivity, leading to socio-economic consequences of loss of life and property, such as reduced workforce participation and strain on public health resources [12]. The stigma associated with the disease can also lead to social isolation, further complicating recovery efforts in affected communities [17].

Mathematical modeling has emerged as a crucial tool for understanding cholera transmission dynamics and evaluating the effectiveness of control measures. Early models by [13] and [7] employed systems of nonlinear differential equations to explore interactions among susceptible, infected and recovered individuals, as well as environmental reservoirs of vibrio cholerae. These foundational work paved way for more sophisticated models that incorporate various public health strategies, including vaccination and sanitation improvement [8, 16]. A mathematical model developed for capturing key cholera dynamics and evaluated for the

[a] *Department of Mathematical Sciences, Osun State University, Osogbo, Nigeria.*
[*] *Correspondence to: M.K. Kolawole. Email: mutairu.kolawole@uniosun.edu.ng*

effectiveness of control strategies such as education, sanitation, treatment and vaccination [9]. The results indicated that, combining multiple strategies significantly enhances control efficacy compared to single intervention.

Recent studies have expanded on these concepts by exploring the role of public awareness in cholera dynamics. For instance, as investigated that the impact of awareness program on transmission rates, revealing that increased public awareness could effectively reduces infection rates. Their work highlight the necessity of incorporating social factors into mathematical models to better reflect real-world dynamics [21]. Additionally, an applied Artificial Neural Networks (ANNs) to forecast cholera incidence in Iran based on climate variables which further demonstrated the intricate relationship between environmental factors and cholera outbreak [18]. Another notable advancement is the development of mathematical model that integrate with physics-informed techniques which represent a novel and powerful advancement in solving complex problem in excelling at learning non-linear mappings between high-dimensional spaces. These networks are especially effective in capturing intricate dynamics and decomposing functions into simpler components, making them ideal for modeling both local and global behaviour in physical systems of ordinary differential equations [1]

The aim of this study is to develop a comprehensive mathematical model that examines the transmission dynamics of cholera while considering environmental influences and public health intervention. By synthesizing insights from existing literature and employing advanced modeling techniques, our research seeks to enhance the understanding of cholera epidemiology and inform effective strategies for outbreak control. Understanding these dynamics is vital for mitigating the socio-economic impacts of cholera, particularly in regions at heightened risk for future outbreaks [10, 2].

1.1. Foundational Concepts

In this section, we present key definitions that are relevant to the present research.

Definition 1 *The Laplace transform of the derivative function $D_tW(t)$ [14, 5] can be expressed as*

$$\mathcal{L}\left[D_tW(t)\right] = s\mathcal{L}\left[W(t)\right] - W(0),$$

where $s \geq 0$ and D_t denotes the standard derivative operator.

Definition 2 *The Adomian polynomials $B_0, B_1, \ldots, B_n$ that facilitate the decomposition of the unknown function $W(t)$, represented as $W(t) = W_0 + W_1 + W_2 + \ldots + W_n$, are defined by:*

$$B_n = \frac{1}{n!}\frac{d^n}{d\lambda^n}\left[H(t)\sum_{j=0}^{n} W_j\lambda^j\right]_{\lambda=0},$$

where $H(t)$ is a nonlinear operator and W_j represents the elements of the decomposition.

2. Methodology

2.1. Laplace Adomian Decomposition Technique

This subsection elaborates on the implementation of the Laplace Adomian Decomposition Technique (LADT) for solving a generalized set of differential equations of integer order, represented as follows:

$$D_tU_k(t) = g_k(U_1, U_2, U_3, U_k) + h_k(U_1, U_2, U_3, U_k), \tag{1}$$

accompanied by the initial condition:

$$U_k(0) = \omega_k, \quad k = 1, 2, 3, ..., r. \tag{2}$$

In equation (1), $D_tU_k(t)$ indicates the standard derivative of the unknown functions $U_k(t)$, where k denotes the index of the terms under consideration. The linear and nonlinear segments of the equation are indicated by g_k and h_k, respectively. Taking the Laplace transform of equation (1) yields:

$$\mathcal{L}\left[D_tU_k(t)\right] = \mathcal{L}\left[g_k(U_1, U_2, U_3, U_k) + h_k(U_1, U_2, U_3, U_k)\right]. \tag{3}$$

Utilizing the properties of the Laplace transform, we derive:

$$s\mathcal{L}[U_k(t)] - U_k(0) = \mathcal{L}\left[g_k(U_1, U_2, U_3, U_k) + h_k(U_1, U_2, U_3, U_k)\right]. \tag{4}$$

According to the Adomian decomposition methodology, $U_k(t)$ can be represented as a series of components:

$$U_k(t) = \sum_{n=0}^{\infty} U_{kn}(t), \quad k = 1, 2, 3, ..., r. \tag{5}$$

Similarly, the nonlinear terms h_k can be decomposed as:

$$h_k(U_1, \ldots, U_k) = \sum_{n=0}^{\infty} A_{kn}(t), \tag{6}$$

where $A_{kn}(t)$ denotes the Adomian polynomials. Substituting equations (5) and (6) into equation (4) yields:

$$s\mathcal{L}\left[\sum_{n=0}^{\infty} U_{kn}(t)\right] = \frac{U_k(0)}{s} + s\mathcal{L}\left[\sum_{n=0}^{\infty} g_{kn}(t)\right] + s\mathcal{L}\left[\sum_{n=0}^{\infty} A_{kn}(t)\right]. \tag{7}$$

Taking the inverse Laplace transform of equation (7) provides the recurrence relation for the solution:

$$U_{k(n+1)}(t) = \mathcal{L}^{-1}\left(\frac{U_k(0)}{s}\right) + \mathcal{L}^{-1}\left[s\mathcal{L}\left[g_k\left(\sum_{n=0}^{\infty} U_{1n}(t), \ldots, \sum_{n=0}^{\infty} U_{kn}(t)\right)\right] + s\mathcal{L}\left[\sum_{n=0}^{\infty} A_{kn}(t)\right]\right]. \tag{8}$$

Simplifying this expression results in:

$$U_{k(n+1)}(t) = c_k + \mathcal{L}^{-1}\left[s\mathcal{L}\left[g_k\left(\sum_{n=0}^{\infty} U_{1n}(t), \ldots, \sum_{n=0}^{\infty} U_{kn}(t)\right)\right] + s\mathcal{L}\left[\sum_{n=0}^{\infty} A_{kn}(t)\right]\right], \tag{9}$$

which represents the required recursive formula for solving the non-fractional differential equation using the Laplace Adomian Decomposition Technique.

2.2. Mathematical model

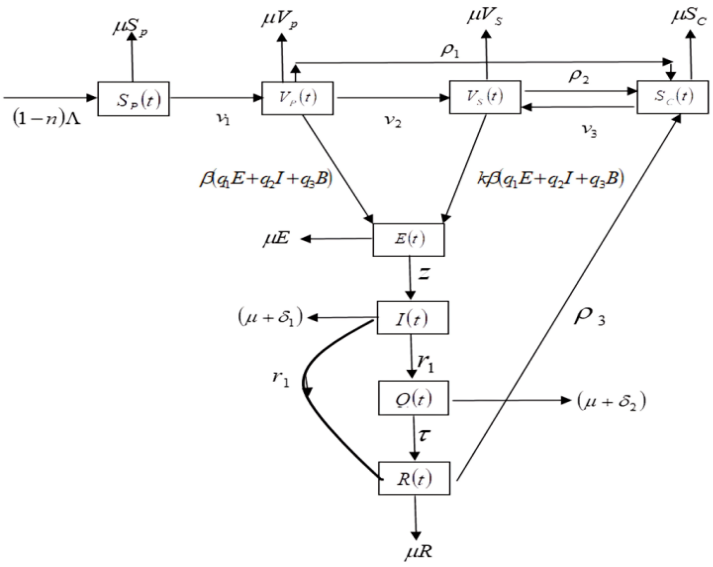

Figure 1. Schematic diagram of the model

The work of Abdulai et al. (2023) was extended by incorporating a vaccine booster administered in two stages: primary vaccination (v_p) and secondary vaccination (v_s), along with a quarantine strategy at Y. This results in a new system of ordinary differential equations that dynamically represents the transmission of cholera fever while assessing the roles of primary, secondary, periodic vaccination and immunity losses. The population is subdivided into various epidemiological classes: Susceptible Primary (S_P), Susceptible Secondary (S_C), Primary Vaccination (V_P), Secondary Vaccination (V_S), Exposed (E), Infected (I), Recovered (R) and a bacteria subclass (B). Recruitment into the susceptible population occurs at a rate denoted as Λ, with vaccinations at different stages occurring at the following rates: infant stage at n, primary stage at v_1, secondary stage at v_2 and periodic booster administration at v_3. Immunity loss rates are given by ρ_1 for the primary stage, ρ_2 for the secondary stage, and ρ_3 for the periodic booster. The rates of infectious transmission are represented as follows: q_1 for exposure, q_2 for infected individuals, and q_3 for bacteria, respectively. Figure 1 gives the schematic diagram of the system of nonlinear differential equations presented in

equation (10) below.

$$\begin{aligned}
\frac{dS_P}{dt} &= (1-n)\Lambda - \beta(q_1E + q_2I + q_3B) - (V_1+\mu)S_P,\\
\frac{dV_P}{dt} &= n\Lambda + V_1S_P - (v_2+p_1+\mu)V_P,\\
\frac{dS_C}{dt} &= (\rho_3+\mu)R + \rho_1V_P + \rho_2V_S - V_3S_C - K\beta(q_1E + q_2I + q_3B)S_C,\\
\frac{dV_S}{dt} &= v_2V_P - (\mu+m)V_S - \rho_2V_S + V_3S_C,\\
\frac{dE}{dt} &= \beta((q_1E + q_2I + q_3B)(S + KS_C) - (\mu+Z)E),\\
\frac{dI}{dt} &= ZE - (\Upsilon_1 + \Upsilon_2 + \mu + \delta_1 + \mu)I,\\
\frac{dQ}{dt} &= \Upsilon_1 I - (\tau + \Upsilon_3 + \delta_2 + \mu)Q,\\
\frac{dR}{dt} &= \Upsilon_2 I + (\tau + \Upsilon_3)Q + mV_S - (\mu+\rho_3)R,\\
\frac{dB}{dt} &= \omega + \xi_1E + \xi_2I - \mu_bB.
\end{aligned} \tag{10}$$

The nomenclature of the model's components are itemized in Table 1 below.

Table 1. Description of Parameters with Baseline Values

Parameter	Description	Baseline Value	Source
S_P	Susceptible primary population	1723	[2]
S_C	Susceptible secondary population	28000	[21]
V_P	Vaccination at primary stage	17621	[1]
V_S	Vaccination at secondary stage	2200	[3]
E	Exposed population	2000	[13, 15]
I	Infected population	130	[16]
R	Recovered population	1.09	[8, 15]
B	Bacteria population	2301	[20]
Λ	Human recruitment rate	168	[14]
n	Fraction of recruited susceptible-vaccinated	0.670	Estimated
β	Transmission rate	0.2713	[1]
q_1	Infectiousness from exposed	1.002	[17]
q_2	Infectiousness from infected	1.001	[6]
q_3	Infectiousness from bacteria	1.01	[4]
ν_1	Vaccination rate at primary stage	0.41	[7]
ν_2	Vaccination rate at secondary stage	0.423	[19]
ν_3	Periodic administration of boosters	0.331	[5, 9]
K	Proportion of susceptible	0.026	[14]
ρ_1	Immunity loss at primary stage	0.2386	[13]
ρ_2	Immunity loss at secondary stage	0.2514	[10]
ρ_3	Immunity loss at periodic stage	0.3237	[11]
μ	Natural mortality rate	0.0041	Estimated
Z	Rate of progression from exposed to infection	0.0000042	[11, 22]
τ	Treatment rate	0.75	Estimated
γ	Recovery rate	0.776	[1]
δ	cholera-induced mortality rate	0.0122	assumed
M	Recovery rate from secondary vaccination	0.0956	assumed
μ_b	Rate of bacteria decay	0.0645	[21]
ω	Growth rate of bacteria	0.01	[16]
ε_1	Rate of bacteria excretion (Exposed)	0.0918	[16]
ε_2	Rate of bacteria excretion (Infected)	0.0812	[19]

3. Model Analysis

In this section, we analyse the basic features of the model

3.1. Positivity and Boundedness of the Solution

In mathematical epidemiology and population dynamics, it is crucial to ensure that all state variables remain positive over time. Positivity is essential for the biological realism of the model, as negative values may lead to nonsensical interpretations. Additionally, establishing positivity helps to confirm the model's well-posedness, indicating that the solution exist, unique and continuously depend on initial condition.

$$\Gamma = \left\{ S_P, S_C, V_P, V_S, E, I, Q, R, B \in \mathbb{R}_+^9 \right\} \tag{11}$$

The initial conditions are defined as follows:

$$\begin{aligned} &S_P(0) = s_{(0)}, \quad S_C(0) = s_{(0)}, \quad V_P(0) = v(0), \\ &V_C(0) = v(0), \quad E(0) = e(0), \quad I(0) = i(0), \\ &Q(0) = q(0), \quad R(0) = r_0, \quad B(0) = b_0 \quad \text{for } t > 0. \end{aligned}$$

Theorem 1 *For the system defined by the parameters in equation (11), the following properties hold:*

1. *All state variables remain positive for $t > 0$.*
2. *The model is well-posed, meaning solution exist, unique and continuously depend on the initial condition.*

s**Proof**
First, consider the equation for $S_P(t)$:

$$\frac{dS_P}{dt} = (1-n)\Lambda - \beta(q_1 E + q_2 I + q_3 B) - (V_1 + \mu)S_P.$$

From this, it can be deduced that:

$$\frac{dS_P}{dt} \geq (V_1 + \mu)S_P(t).$$

By separating variables, it is obtained that :

$$\frac{dS_P}{S_P(t)} \geq -(V_1 + \mu)dt.$$

Integrating both sides result in:

$$\int \frac{dS_P}{S_P(t)} \geq -(V_1 + \mu)\int dt.$$

Thus,

$$S_P(t) \geq -(V_1 + \mu)t + c.$$

This implies:

$$S_P(t) \geq e^{-(V_1+\mu)t+c} \geq S_P(0)e^{-(V_1+\mu)t+C} > 0,$$

where $S_P(0) = e^c$. Next, it can be analysed that $V_P(t)$:

$$\frac{dV_P}{dt} = n\Lambda + V_1 S - (V_2 + P_1 + \mu)V_P.$$

Thus:

$$\frac{dV_P}{dt} \geq n\Lambda + V_1 S - (V_2 + P_1 + \mu)V_P.$$

Using the variable separable method:

$$\frac{dV_P}{V_P(t)} \geq -(V_2 + P_1 + \mu).$$

Integrating gives:

$$\int \frac{dV_P}{dt} \geq -(V_2 + P_1 + \mu)\int dt.$$

This leads to:

$$V_P(t) \geq e^{-(V_2+\mu+P_1)t+c} \geq V_P(0)e^{-(V_2+\mu+P_1)t+c} > 0.$$

Lastly, consider $S_C(t)$:

$$\frac{dS_C}{dt} = (\rho_3 + \mu)R + \rho_1 V_P + \rho_2 V_S - V_3 S_C - K\beta(q_1 E + q_2 I + q_3 B)S_C.$$

It is obtained that:

$$\frac{dS_C}{dt} \geq (\rho_3 + \mu)R + \rho_1 V_P + \rho_2 V_S - V_3 S_C - K\beta(q_1 E + q_2 I + q_3 B)S_C.$$

Separating variables yields:

$$\frac{dS_C}{S_C(t)} \geq -K\beta(q_1 E + q_2 I + q_3 B).$$

Integrating gives:

$$\int \frac{dS_C}{S_C(t)} \geq -K\beta(q_1 E + q_2 I + q_3 B) \int dt.$$

Thus, it can be deduced that:

$$S_C(t) \geq -K\beta(q_1 E + q_2 I + q_3 B)t + c.$$

This shows that:

$$S_C(t) \geq S(0)e^{-K\beta(q_1 E + q_2 I + q_3 B)t + c} > 0.$$

for the exposed population $E(t)$:

$$\frac{dE}{dt} = \beta\left((q_1 E + q_2 I + q_3 B)(S + KS_C) - (\mu + Z)E\right)$$

it can be asserted that:

$$\frac{dE}{dt} \geq -(\mu + Z)E(t)$$

Dividing through by $E(t)$:

$$\frac{dE}{E(t)} \geq -(\mu + Z)dt$$

Integrating yields:

$$\int \frac{dE}{E(t)} \geq -(\mu + Z) \int dt$$

Thus is is resolved that:

$$E(t) \geq e(0)e^{-(\mu+Z)t+c} > 0$$

Next, for the infected population $I(t)$:

$$\frac{dI}{dt} = ZE - (\Upsilon_1 + \Upsilon_2 + \mu + \delta_1)I$$

This leads us to:

$$\frac{dI}{dt} \geq -(\Upsilon_1 + \Upsilon_2 + \mu + \delta_1)I$$

Again, dividing through by $I(t)$:

$$\frac{dI}{I(t)} \geq -(\Upsilon_1 + \Upsilon_2 + \mu + \delta_1)dt$$

Integrating gives:

$$\int \frac{dI}{I(t)} \geq -(\Upsilon_1 + \Upsilon_2 + \mu + \delta_1) \int dt$$

Thus is is resolved that:

$$I(t) \geq i(0)e^{-(\Upsilon_1+\Upsilon_2+\mu+\delta_1)t} > 0$$

For the quarantined population $Q(t)$:

$$\frac{dQ}{dt} = \Upsilon_1 I - (\tau + \Upsilon_3 + \delta_2 + \mu)Q$$

We derive:

$$\frac{dQ}{dt} \geq -(\tau + \Upsilon_3 + \delta_2 + \mu)Q$$

This yields:

$$\frac{dQ}{Q(t)} \geq -(\tau + \Upsilon_3 + \delta_2 + \mu)dt$$

Integrating result in:

$$\int \frac{dQ}{Q(t)} \geq -(\tau + \Upsilon_3 + \delta_2 + \mu) \int dt$$

it is resolved that

$$Q(t) \geq q(0)e^{-(\tau+\Upsilon_3+\delta_2+\mu)t} > 0$$

Next, for the carrier state $S_C(t)$:

$$\frac{dS_C}{dt} = (\rho_3 + \mu)R + \rho_1 V_P + \rho_2 V_S - V_3 S_C - K\beta(q_1 E + q_2 I + q_3 B)S_C$$

It is derived that:

$$\frac{dS_C}{dt} \geq -K\beta(q_1 E + q_2 I + q_3 B)S_C$$

This result in:

$$\frac{dS_C}{S_C} \geq -K\beta(q_1 E + q_2 I + q_3 B)dt$$

Integrating gives:

$$\int \frac{dS_C}{S_C} \geq -K\beta(q_1 E + q_2 I + q_3 B) \int dt$$

Thus:

$$S_C(t) \geq s_C(0)e^{-K\beta(q_1 E+q_2 I+q_3 B)t} > 0$$

Finally, for the recovered population $R(t)$:

$$\frac{dR}{dt} = \Upsilon_2 I + (\tau + \Upsilon_3)Q + mV_S - (\mu + \rho_3)R$$

To derive:

$$\frac{dR}{dt} \geq -(\mu + \rho_3)R(t)$$

This leads to:

$$\frac{dR}{R(t)} \geq -(\mu + \rho_3)dt$$

Integrating gives:

$$\int \frac{dR}{R(t)} \geq -(\mu + \rho_3) \int dt$$

It is concluded that:

$$R(t) \geq r(0)e^{-(\mu+\rho_3)t} > 0$$

Consequently, since all variables in R_9^+ at equilibrium defined by the model function, represent well-posed mathematical and epidemiological problems, It is affirmed that the solutions are positively invariant. As a result, all state variables remain positive for $t > 0$ and the model is well-posed.

3.2. Existence and Uniqueness of the Model

To assess the existence and uniqueness of solution for the model, we begin by defining the following functions from equation (10)

$$
\begin{aligned}
F_1 &= (1-n)\Lambda - \beta(q_1E + q_2I + q_3B) - (V_1+\mu)S_P,\\
F_2 &= n\Lambda + V_1S_P - (v_2+p_1+\mu)V_P,\\
F_3 &= (\rho_3+\mu)R + \rho_1V_P + \rho_2V_S - V_3S_C - K\beta(q_1E + q_2I + q_3B)S_C,\\
F_4 &= v_2V_P - (\mu+m)V_S - \rho_2V_S + V_3S_C,\\
F_5 &= \beta((q_1E + q_2I + q_3B)(S + KS_C) - (\mu+Z)E),\\
F_6 &= ZE - (\Upsilon_1 + \Upsilon_2 + \mu + \delta_1 + \mu)I,\\
F_7 &= \Upsilon_1 I - (\tau + \Upsilon_3 + \delta_2 + \mu)Q,\\
F_8 &= \Upsilon_2 I + (\tau + \Upsilon_3)Q + mV_S - (\mu+\rho_3)R,\\
F_9 &= \omega + \xi_1E + \xi_2I - \mu_bB.
\end{aligned}
\tag{12}
$$

Analysing these functions to establish the existence and uniqueness of the model solutions are given below.

$$
\begin{aligned}
&\left|\frac{\partial F_1}{\partial S}\right| = V_1+\mu, && \left|\frac{\partial F_1}{\partial S_C}\right| = 0, && \left|\frac{\partial F_1}{\partial V_P}\right| = 0,\\
&\left|\frac{\partial F_1}{\partial V_S}\right| = 0, && \left|\frac{\partial F_1}{\partial E}\right| = \beta q_1, && \left|\frac{\partial F_1}{\partial I}\right| = \beta q_2,\\
&\left|\frac{\partial F_1}{\partial R}\right| = 0, && \left|\frac{\partial F_1}{\partial Q}\right| = 0, && \left|\frac{\partial F_1}{\partial B}\right| = \beta q_3,\\
&\left|\frac{\partial F_2}{\partial V_P}\right| = V_2+\rho_1+\mu, && \left|\frac{\partial F_2}{\partial S_P}\right| = 0, && \left|\frac{\partial F_2}{\partial S_C}\right| = 0,\\
&\left|\frac{\partial F_2}{\partial V_S}\right| = V_1, && \left|\frac{\partial F_2}{\partial E}\right| = 0, && \left|\frac{\partial F_2}{\partial I}\right| = 0,\\
&\left|\frac{\partial F_2}{\partial Q}\right| = 0, && \left|\frac{\partial F_2}{\partial R}\right| = 0, && \left|\frac{\partial F_2}{\partial B}\right| = 0,\\
&\left|\frac{\partial F_3}{\partial S_P}\right| = 0, && \left|\frac{\partial F_3}{\partial S_C}\right| = V_3 + K\beta(q_1+q_2+q_3), && \left|\frac{\partial F_3}{\partial V_P}\right| = P_1,\\
&\left|\frac{\partial F_3}{\partial V_S}\right| = P_2, && \left|\frac{\partial F_3}{\partial E}\right| = K\beta q_1, && \left|\frac{\partial F_3}{\partial I}\right| = K\beta q_2,\\
&\left|\frac{\partial F_3}{\partial Q}\right| = 0, && \left|\frac{\partial F_3}{\partial R}\right| = \rho_3+\mu, && \left|\frac{\partial F_3}{\partial B}\right| = 0,\\
&\left|\frac{\partial F_4}{\partial S_P}\right| = 0, && \left|\frac{\partial F_4}{\partial S_C}\right| = V_3, && \left|\frac{\partial F_4}{\partial V_P}\right| = V_2,\\
&\left|\frac{\partial F_4}{\partial V_S}\right| = P_2, && \left|\frac{\partial F_4}{\partial E}\right| = 0, && \left|\frac{\partial F_4}{\partial I}\right| = 0,\\
&\left|\frac{\partial F_4}{\partial Q}\right| = 0, && \left|\frac{\partial F_4}{\partial R}\right| = 0, && \left|\frac{\partial F_4}{\partial B}\right| = 0,\\
&\left|\frac{\partial F_5}{\partial S_P}\right| = \beta(q_1+q_2+q_3+K), && \left|\frac{\partial F_5}{\partial S_C}\right| = K, && \left|\frac{\partial F_5}{\partial V_P}\right| = 0,\\
&\left|\frac{\partial F_5}{\partial V_S}\right| = 0, && \left|\frac{\partial F_5}{\partial E}\right| = \beta q_1+\mu+z, && \left|\frac{\partial F_5}{\partial I}\right| = \beta q_2,\\
&\left|\frac{\partial F_5}{\partial Q}\right| = 0, && \left|\frac{\partial F_5}{\partial R}\right| = 0, && \left|\frac{\partial F_5}{\partial B}\right| = \beta q_2,\\
&\left|\frac{\partial F_6}{\partial S_P}\right| = 0, && \left|\frac{\partial F_6}{\partial S_C}\right| = 0, && \left|\frac{\partial F_6}{\partial V_P}\right| = 0,\\
&\left|\frac{\partial F_6}{\partial V_S}\right| = 0, && \left|\frac{\partial F_6}{\partial E}\right| = Z, && \left|\frac{\partial F_6}{\partial I}\right| = Y,\\
&\left|\frac{\partial F_6}{\partial Q}\right| = 0, && \left|\frac{\partial F_6}{\partial B}\right| = 0, && \left|\frac{\partial F_6}{\partial R}\right| = 0.
\end{aligned}
$$

$$\left|\frac{\partial F_6}{\partial S_C}\right| = 0, \quad \left|\frac{\partial F_6}{\partial V_P}\right| = 0, \quad \left|\frac{\partial F_6}{\partial V_S}\right| = 0, \quad \left|\frac{\partial F_6}{\partial E}\right| = Z, \quad \left|\frac{\partial F_6}{\partial I}\right| = Y,$$
$$\left|\frac{\partial F_6}{\partial Q}\right| = 0, \quad \left|\frac{\partial F_6}{\partial B}\right| = 0, \quad \left|\frac{\partial F_6}{\partial R}\right| = 0,$$
$$\left|\frac{\partial F_7}{\partial S_P}\right| = 0, \quad \left|\frac{\partial F_7}{\partial V_P}\right| = 0, \quad \left|\frac{\partial F_7}{\partial S_C}\right| = 0, \quad \left|\frac{\partial F_7}{\partial V_S}\right| = 0, \quad \left|\frac{\partial F_7}{\partial E}\right| = 0,$$
$$\left|\frac{\partial F_7}{\partial I}\right| = \Upsilon_1, \quad \left|\frac{\partial F_7}{\partial Q}\right| = -(\tau + \Upsilon_3 + \delta_2 + \mu), \quad \left|\frac{\partial F_7}{\partial R}\right| = 0, \quad \left|\frac{\partial F_7}{\partial B}\right| = 0,$$
$$\left|\frac{\partial F_8}{\partial S_P}\right| = 0, \quad \left|\frac{\partial F_8}{\partial V_P}\right| = 0, \quad \left|\frac{\partial F_8}{\partial S_C}\right| = 0, \quad \left|\frac{\partial F_8}{\partial V_S}\right| = m, \quad \left|\frac{\partial F_8}{\partial E}\right| = 0,$$
$$\left|\frac{\partial F_8}{\partial I}\right| = \Upsilon_2, \quad \left|\frac{\partial F_8}{\partial Q}\right| = \tau + \Upsilon_3, \quad \left|\frac{\partial F_8}{\partial R}\right| = -(\mu + \rho_3), \quad \left|\frac{\partial F_8}{\partial B}\right| = 0,$$
$$\left|\frac{\partial F_9}{\partial S_P}\right| = 0, \quad \left|\frac{\partial F_9}{\partial V_P}\right| = 0, \quad \left|\frac{\partial F_9}{\partial S_C}\right| = 0, \quad \left|\frac{\partial F_9}{\partial V_S}\right| = 0, \quad \left|\frac{\partial F_9}{\partial E}\right| = \xi_1,$$
$$\left|\frac{\partial F_9}{\partial I}\right| = \xi_2, \quad \left|\frac{\partial F_9}{\partial Q}\right| = 0, \quad \left|\frac{\partial F_9}{\partial R}\right| = 0, \quad \left|\frac{\partial F_9}{\partial B}\right| = -\mu_b.$$

These examination of the computed partial derivatives $\left|\frac{\partial F_i}{\partial x_j}\right|$ confirms that each function F_i is continuous and differentiable concerning the state variables S_P, S_C, V_P, V_S, E, I, R, Q, and B. These results indicate that the existence and uniqueness of the solution which affirms a well- defined nature of the system under investigation.

3.3. The disease free equilibrium

The disease free equilibrium is a state where the disease is absent in the population, and the system stabilizes without any infected individuals.
Let disease free equilibrium be represented by $\text{DFE}_0(S_{p0}, S_{C0}, V_{P0}, V_{S0}, E_0, I_0, R_0, B_0)$ and equate the system of equation (10) to zero, substituting $S_p = S_{p0}, S_c = S_{C0}, V_p = V_{p0}, V_S = V_{S0}, E = E_0 = 0, I = I_0 = 0, R = R_0 = 0, B = B_0 = 0$.

Solving the remaining equations, we have:

$$\begin{gathered}(1-n)\Lambda - \beta(q_1E + q_2I + q_3B) - (\nu_1 + \mu)S_P = 0\\ (\rho_3 + \mu)R + \rho_1V_P + \rho_2V_S - \nu_3S_C - K\beta(q_1E + q_2I + q_3B)S_C = 0\\ n\Lambda + \nu_1S_P - (\nu_2 + \rho_1 + \mu)V_P = 0\\ \nu_2V_P - (\mu + m)V_S - \rho_2V_S + \nu_3S_C = 0\end{gathered} \tag{13}$$

From the first equation of (13):

$$\begin{gathered}(1-n)\Lambda - \beta(q_1E + q_2I + q_3B) - (\nu_1 + \mu)S_P = 0\\ (1-n)\Lambda = (\nu_1 + \mu)S_P\\ S_P = \frac{(1-n)\Lambda}{(\nu_1 + \mu)}\end{gathered} \tag{14}$$

From the second equation of (13):

$$\begin{gathered}(\rho_3 + \mu)R + \rho_1V_P + \rho_2V_S - \nu_3S_C - K\beta(q_1E + q_2I + q_3B)S_C = 0\\ \rho_1V_P + \rho_2V_S - \nu_3S_C = 0\\ \rho_1V_P + \rho_2V_S = \nu_3S_C\\ S_C = \frac{\rho_1V_P + \rho_2V_S}{\nu_3}\end{gathered} \tag{15}$$

From the third equation of (13):

$$\begin{gathered}n\Lambda + \nu_1S_P - (\nu_2 + \rho_1 + \mu)V_P = 0\\ n\Lambda + \nu_1S_P = (\nu_2 + \rho_1 + \mu)V_P\\ V_P = \frac{n\Lambda + \nu_1S_P}{(\nu_2 + \rho_1 + \mu)}\end{gathered} \tag{16}$$

From the last equation of (13):

$$\nu_2V_P - (\mu + m)V_S - \rho_2V_S + \nu_3S_C = 0$$

$$\nu_2 V_P + \nu_3 S_C = (\mu + m)V_S + \rho_2 V_S$$

$$V_S = \frac{\nu_2 V_P + \nu_3 S_C}{(\mu + m) + \rho_2} \tag{17}$$

$$E_0 = \{S_{P_0}, S_{C_0}, V_{P_0}, V_{S_0}, E_0, I_0, R_0, B_0\} = \left\{\frac{(1-n)\Lambda}{(\nu_1+\mu)}, \frac{\rho_1 V_P + \rho_2 V_S}{\nu_3}, \frac{n\Lambda + \nu_1 S_P}{(\nu_2+\rho_1+\mu)}, \frac{\nu_2 V_P + \nu_3 S_C}{(\mu+m)+\rho_2}, 0, 0, 0, 0\right\} \tag{18}$$

Endemic Equilibrium Analysis

To identify the endemic equilibrium state for the model, we begin by setting each time derivative to zero, reflecting the stable condition where all variables remain constant over time:

$$\frac{dS_P}{dt} = \frac{dV_P}{dt} = \frac{dS_C}{dt} = \frac{dV_S}{dt} = \frac{dE}{dt} = \frac{dI}{dt} = \frac{dQ}{dt} = \frac{dR}{dt} = \frac{dB}{dt} = 0.$$

Thus, solving for the endemic equilibrium values denoted by S_P^*, V_P^*, S_C^*, V_S^*, E^*, I^*, Q^*, R^*, and B^* sequentially by making substitutions where applicable we have:

$$I^* = \frac{ZE^*}{\Upsilon_1 + \Upsilon_2 + \delta_1 + \mu}.$$

$$Q^* = \frac{\Upsilon_1 I^*}{\tau + \Upsilon_3 + \delta_2 + \mu}.$$

$$R^* = \frac{\Upsilon_2 I^* + (\tau + \Upsilon_3)Q^* + mV_S^*}{\mu + \rho_3}.$$

$$B^* = \frac{\xi_1 E^* + \xi_2 I^*}{\mu_b}.$$

$$E^* = \frac{\beta(q_1 E^* + q_2 I^* + q_3 B^*)(S_P^* + KS_C^*)}{\mu + Z}.$$

$$V_S^* = \frac{V_2 V_P^* + V_3 S_C^*}{\mu + m + \rho_2}.$$

$$S_C^* = \frac{(\rho_3 + \mu)R^* + \rho_1 V_P^* + \rho_2 V_S^*}{V_3 + K\beta(q_1 E^* + q_2 I^* + q_3 B^*)}.$$

$$V_P^* = \frac{n\Lambda + V_1 S_P^*}{V_2 + p_1 + \mu}.$$

$$S_P^* = \frac{(1-\pi)\Lambda}{\beta(q_1 E^* + q_2 I^* + q_3 B^*) + V_1 + \mu}.$$

3.4. The Basic Reproduction Number

The basic reproduction number, R_0, represents the average number of secondary infections caused by a single infected individual in a fully susceptible population. It is crucial for assessing the potential spread of an infection. Using the next-generation matrix method, R_0 is calculated by distinguishing between new infections and the transition between stages of infection.
We start by defining the infection matrix F, which captures new infections, and the transition matrix V, representing the transitions through different stages of infection:

$$F = \begin{pmatrix} \beta q_1(S_P + KS_C) & \beta q_2(S_P + KS_C) & 0 & \beta q_3(S_P + KS_C) \\ 0 & 0 & 0 & 0 \\ 0 & 0 & 0 & 0 \\ 0 & 0 & 0 & 0 \end{pmatrix}$$

$$V = \begin{pmatrix} (\mu + z) & 0 & 0 & 0 \\ -z & (\tau + \gamma + \mu + \delta) & 0 & 0 \\ 0 & -\Upsilon_1 & (\tau + \Upsilon_3 + \delta_2 + \mu) & 0 \\ -\varepsilon_1 & -\varepsilon_2 & 0 & \mu_b \end{pmatrix}$$

The basic reproduction number R_0 is then derived as the spectral radius of FV^{-1}:

$$R_0 = \frac{\beta\left(q_1 + q_2\frac{z}{\tau+\gamma+\mu+\delta} + q_3\frac{\varepsilon_2}{\mu_b}\right)(S_P + KS_C)}{(\mu+z)}$$

Additionally, a related expression captures further details of transmission dynamics:

$$R_0 = \frac{\beta q_1(S_P + KS_C)(\tau+\Upsilon_3+\mu+\delta_2)\mu_b}{(\tau+\Upsilon_3+\mu+\delta_2)} = \frac{\beta q_1\left(\frac{(1-n)\lambda}{(V_1+\mu^+)} + \frac{K\beta_1V_2+\varepsilon_2V_3}{V_2}\right)}{(\tau+\Upsilon_3+\mu+\delta_2)}$$

If $R_0 > 1$, the infection spreads; if $R_0 < 1$, it dies out. This compact formula offers insight into the influence of transmission rates, susceptible populations and recovery or progression rates on disease dynamics.

3.5. Local Stability of disease free equilibrium Point

The disease free equilibrium of the cholera epidemic model is locally asymptotically stable if all eigenvalues of the Jacobian matrix $|JE_1 - \lambda_1| = 0$, $\lambda_i \leq 0$ else unstable. Since

$$E_1 = \left\{\frac{(1-n)\Lambda}{(\nu_1+\mu)}, \frac{\rho_1V_P + \rho_2V_S}{\nu_3}, \frac{n\Lambda + \nu_1S_P}{(\nu_2+\rho_1+\mu)}, \frac{\nu_2V_P + \nu_3S_C}{(\mu+m)+\rho_2}, 0, 0, 0, 0\right\}$$

The Jacobian matrix of the system at E_1 is given by

$$JE_0 = \begin{vmatrix} -(V_1+\mu) & 0 & 0 & -\beta q_1 & -\beta q_2 & 0 & 0 & 0 & -\beta q_3 \\ V_1 & -(V_2+P_1+\mu) & 0 & 0 & 0 & 0 & 0 & 0 & 0 \\ 0 & 0 & 0 & -(\mu+m+P_2) & 0 & 0 & 0 & V_3 & 0 \\ 0 & 0 & 0 & 0 & -(\mu+Z) & \beta q_2 & 0 & K & 0 \\ 0 & 0 & 0 & 0 & Z & -(Y_1+Y_2+\mu+\delta_1) & 0 & 0 & 0 \\ 0 & 0 & 0 & 0 & 0 & Y_1 & -(Y_3+\mu+\delta_2) & 0 & 0 \\ 0 & P_1 & P_2 & -K\beta q_1 & -K\beta q_2 & 0 & -(K\beta(q_1+q_2+q_3)+\mu) & 0 & \\ 0 & 0 & m & 0 & Y_2 & \tau+Y_3 & 0 & -(\mu+P_3) & 0 \\ 0 & 0 & 0 & 0 & 0 & \varepsilon_1 & \varepsilon_2 & 0 & -\mu_b \end{vmatrix}$$

and the eigenvalues are obtained as

$$\lambda_1 = -(V_1+\mu), \quad \lambda_2 = -(V_2+P_1+\mu), \quad \lambda_3 = -(\mu+m+P_2), \quad \lambda_4 = -(\mu+Z),$$
$$\lambda_5 = -(Y_1+Y_2+\mu+\delta_1), \quad \lambda_6 = -(\tau+Y_3+\mu+\delta_2), \quad \lambda_7 = -K\beta(q_1+q_2+q_3), \quad \lambda_8 = -(\mu+P_3), \quad \lambda_9 = -\mu_b.$$

Thus, the disease free equilibrium is locally asymptotically stable since all eigenvalues $\lambda_1, \ldots, \lambda_9$ are negative.

3.6. Sensitivity Analysis of R_0

This subsection conducts a sensitivity analysis of the basic reproduction number R_0 by differentiating R_0 with respect to all its parameters and evaluating the results using the baseline values of the parameters listed in Table 1. The normalized forward sensitivity index is defined as:

$$\gamma_P = \frac{\partial R_0}{\partial P} \times \frac{P}{R_0} \tag{19}$$

where S_{R_0} is the sensitivity index, x_i represents the parameter of interest, and R_0 given by

$$\frac{\beta q_1\left(\frac{(1-n)\lambda}{(V_1+\mu^+)} + \frac{K\beta_1V_2+\varepsilon_2V_3}{V_2}\right)}{(\tau+\Upsilon_3+\mu+\delta_2)} \tag{20}$$

the sensitivity indices of the basic reproduction number for the model are presented in Table 2. The results provide insights into how variations in each parameter affect R_0.

Table 2. Sensitivity analysis of parameters and indices

Parameter	Sensitivity
Ω	-1.278688525
η	1.00000000
ψ_1	$3.738474319 \times 10^{-3}$
ψ_2	$2.610142447 \times 10^{-3}$
G	$9.2234591679 \times 10^{-3}$
ν	0.79965
τ	$8.116508333 \times 10^{-7}$
δ	0.017140282
μ	0.004647773279
ρ_1	$2.00004182 \times 10^{-4}$
ρ_2	$2.193040109 \times 10^{-4}$

The sensitivity analysis presented highlights the influence of various parameters on disease dynamics. Notably, Ω has a negative sensitivity of -1.278688525, indicating that reduction in this parameter can escalate disease prevalence, underscoring its importance in disease control. Conversely, η displays high sensitivity (1.00000000), suggesting that it is a crucial parameter for effective intervention strategies. Parameters like τ (treatment rate) exhibit minimal sensitivity ($8.116508333 \times 10^{-7}$), indicating low impact on disease dynamics but still warrant monitoring for overall effectiveness. The low sensitivity values for immunity loss rates, ρ_1 and ρ_2, suggest their minor immediate effects, yet they remain important for long-term control strategies. Overall, the analysis underscores the necessity for targeted interventions which focus on high-sensitive parameters to optimize public health efforts and improve disease management outcome.

3.7. Model Solution via Laplace Adomian Decomposition Method

From the first equation of the system given by (64), we have

$$\frac{dS_P}{dt} = (1-n)\Lambda - \beta(q_1E + q_2I + q_3B) - (\nu_1 + \mu)S_P.$$

Next, we take the Laplace transform:

$$\eta L\left[S_P(t) - S_P(0)\right] = L\left[(1-n)\Lambda - \beta(q_1E + q_2I + q_3B) - (\nu_1 + \mu)S_P\right]. \tag{21}$$

This can be expressed as:

$$L\left[S_P(t)\right] = \frac{s_P(0)}{\eta} + \frac{L}{\eta}\left[(1-n)\Lambda - \beta(q_1E + q_2I + q_3B) - (\nu_1 + \mu)S_P\right].$$

Since $S_P(0) = s_{P0}$, $E(0) = e_0$, $I(0) = i_0$, $B(0) = b_0$, we can rewrite it as:

$$L\left[S_P(t)\right] = \frac{s_{P0}}{\eta} + \frac{L}{\eta}\left[(1-n)\Lambda - \beta(q_1E + q_2I + q_3B) - (\nu_1 + \mu)S_P\right].$$

Taking the inverse Laplace transform yields:

$$L^{-1}\left\{L\left[S_P(t)\right]\right\} = L^{-1}\left\{\frac{s_{P0}}{\eta} + \frac{L}{\eta}(1-n)\Lambda\right\} - L^{-1}\left\{\frac{L}{\eta}\left[\beta(q_1E + q_2I + q_3B) - (\nu_1 + \mu)S_P\right]\right\}. \tag{22}$$

Thus, we have:

$$S_P(t) = L^{-1}\left\{\frac{s_{P0}}{\eta} + \frac{L}{\eta}(1-n)\Lambda\right\} - L^{-1}\left\{\frac{L}{\eta}\left[\beta(q_1E + q_2I + q_3B) - (\nu_1 + \mu)S_P\right]\right\}.$$

This can be simplified to:

$$S_P(t) = S_{P0} + (1-n)\Lambda t^2 - L^{-1}\left\{\frac{L}{\eta}\left[\beta(q_1E + q_2I + q_3B) - (\nu_1 + \mu)S_P\right]\right\}.$$

Next, applying Adomian decomposition, we express $S_P(t)$ as follows:

$$S_P(t) = S_{P0}(t) + S_{P1}(t) + S_{P2}(t) + \ldots + S_{Pn}(t) = \sum_{n=0}^{\infty} S_{Pn}(t).$$

This leads to:

$$\sum_{n=0}^{\infty} S_{Pn}(t) = S_{P0} + (1-n)\Lambda t^2 - L^{-1}\left\{\frac{L}{\eta}\left[\beta\left(q_1\sum_{n=0}^{\infty}E_n + q_2\sum_{n=0}^{\infty}I_n + q_3\sum_{n=0}^{\infty}B_n\right) - (\nu_1 + \mu)\sum_{n=0}^{\infty}S_{Pn}\right]\right\}. \tag{23}$$

Initial Approximation:

$$S_{P0}(t) = s_{P0} + (1-n)\Lambda t^2, \quad E_0(t) = e_0, \quad I_0(t) = i_0, \quad B_0(t) = b_0.$$

Recurrence Formula:

$$\sum_{n=0}^{\infty} S_{P_{n+1}}(t) = -L^{-1}\left\{\frac{L}{\eta}\left[\beta\left(q_1\sum_{n=0}^{\infty}E_n + q_2\sum_{n=0}^{\infty}I_n + q_3\sum_{n=0}^{\infty}B_n\right) - (\nu_1 + \mu)\sum_{n=0}^{\infty}S_{Pn}\right]\right\}. \tag{24}$$

First Iteration (when $n = 0$):

$$S_{P1}(t) = -L^{-1}\left\{\frac{L}{\eta}\left[\beta\left(q_1e_0 + q_2i_0 + q_3b_0\right) - (\nu_1 + \mu)(s_{P0} + (1-n)\Lambda t^2)\right]\right\}.$$

This expression can be simplified to:

$$S_{P1}(t) = L^{-1}\left\{\frac{(\nu_1+\mu)s_{P0}}{\eta^2} - \frac{\beta\left(q_1e_0+q_2i_0+q_3b_0\right)}{\eta^3} - \frac{(\nu_1+\mu)(1-n)\Lambda}{\eta^4}\right\}.$$

Thus, we derive the following:

$$S_{P1}(t) = (\nu_1+\mu)s_{P0}t - \beta\left(q_1e_0+q_2i_0+q_3b_0\right)t^2 - (\nu_1+\mu)(1-n)\Lambda t^3. \tag{25}$$

In same manner from the second variable in (25) above

$$\frac{dS_C}{dt} = (\rho_3+\mu)R + \rho_1V_P + \rho_2V_S - \nu_3S_C - K\beta(q_1E+q_2I+q_3B)S_C. \tag{26}$$

Taking the Laplace transform, we get:

$$L\left[\frac{dS_C}{dt}\right] = L\left[(\rho_3+\mu)R + \rho_1V_P + \rho_2V_S - \nu_3S_C - K\beta(q_1E+q_2I+q_3B)S_C\right]. \tag{27}$$

This leads us to:

$$\eta L\{S_C(t)\} - S_C(0) = L\left[(\rho_3+\mu)R + \rho_1V_P + \rho_2V_S - \nu_3S_C - K\beta(q_1E+q_2I+q_3B)S_C\right]. \tag{28}$$

Thus, we can express $L\{S_C(t)\}$ as:

$$L\{S_C(t)\} = \frac{S_C(0)}{\eta} + \frac{L}{\eta}\left[(\rho_3+\mu)R + \rho_1V_P + \rho_2V_S - \nu_3S_C - K\beta(q_1E+q_2I+q_3B)S_C\right]. \tag{29}$$

Now, taking the inverse Laplace transform yields:

$$L^{-1}\left[L\{S_C(t)\}\right] = L^{-1}\left[\frac{S_C(0)}{\eta}\right] + L^{-1}\left[\frac{L}{\eta}\left[(\rho_3+\mu)R + \rho_1V_P + \rho_2V_S - \nu_3S_C - K\beta(q_1E+q_2I+q_3B)S_C\right]\right]. \tag{30}$$

Therefore, we can express $S_C(t)$ as:

$$S_C(t) = L^{-1}\left[\frac{S_C(0)}{\eta}\right] + L^{-1}\left[\frac{L}{\eta}\left[(\rho_3+\mu)R + \rho_1V_P + \rho_2V_S - \nu_3S_C - K\beta(q_1E+q_2I+q_3B)S_C\right]\right]. \tag{31}$$

Since $S_C(0) = s_{c0}$, we can rewrite:

$$S_C(t) = L^{-1}\left[\frac{s_{c0}}{\eta}\right] + L^{-1}\left[\frac{L}{\eta}\left[(\rho_3+\mu)R + \rho_1V_P + \rho_2V_S - \nu_3S_C - K\beta(q_1E+q_2I+q_3B)S_C\right]\right]. \tag{32}$$

Thus, we have:

$$S_C(t) = s_{c0} + L^{-1}\left[\frac{L}{\eta}\left[(\rho_3+\mu)R + \rho_1V_P + \rho_2V_S - \nu_3S_C - K\beta(q_1E+q_2I+q_3B)S_C\right]\right]. \tag{33}$$

For the Adomian Decomposition, we express:

$$S_C(t) = S_{C0}(t) + S_{C1}(t) + S_{C2}(t) + \ldots + S_{Cn}(t) = \sum_{n=0}^{\infty} S_{Cn}(t). \tag{34}$$

This leads us to:

$$\sum_{n=0}^{\infty} S_{C_{n+1}}(t) = s_{c0} + L^{-1}\left[\frac{L}{\eta}\left[(\rho_3+\mu)R + \rho_1V_P + \rho_2V_S - \nu_3S_C - K\beta(q_1E+q_2I+q_3B)S_C\right]\right]. \tag{35}$$

The initial approximations are defined as follows:

$$S_{C0}(t) = s_{c0}, \quad E_0(t) = e_0, \quad I_0(t) = i_0, B_0(t) = b_0, \quad R_0(t) = R_0, \quad V_{P0}(t) = v_{p0} + n\Lambda t^2, \quad V_{S0}(t) = v_{s0}.$$

The recurrence formula is expressed as:

$$\sum_{n=0}^{\infty} S_{C_{n+1}}(t) = L^{-1}\left[\frac{L}{\eta}\left[\begin{array}{l}(\rho_3+\mu)\sum_{n=0}^{\infty}R_n + \rho_1\sum_{n=0}^{\infty}V_{P,n} + \rho_2\sum_{n=0}^{\infty}V_{S,n} \\ -\nu_3\sum_{n=0}^{\infty}S_{C,n} - K\beta\left(q_1\sum_{n=0}^{\infty}E_n + q_2\sum_{n=0}^{\infty}I_n + q_3\sum_{n=0}^{\infty}B_n\right)\sum_{n=0}^{\infty}S_{C,n}\end{array}\right]\right]. \tag{36}$$

From the initial approximation, when $n = 0$, we can express $S_{C1}(t)$ as follows:

$$S_{C1}(t) = L^{-1}\left[\frac{L}{\eta}\left[\begin{array}{l}(\rho_3+\mu)r_0+\rho_1 v_{P0}+\rho_2 v_{S0}-\nu_3 s_{C0}\\ -K\beta(q_1 e_0+q_2 i_0+q_3 b_0)s_{C0}\end{array}\right]\right]$$

This can be rewritten, incorporating $n\Lambda t^2$:

$$S_{C1}(t) = L^{-1}\left[\frac{L}{\eta}\left[\begin{array}{l}(\rho_3+\mu)r_0+\rho_1(v_{P0}+n\Lambda t^2)+\rho_2 v_{S0}-\nu_3 s_{C0}\\ -K\beta(q_1 e_0+q_2 i_0+q_3 b_0)s_{C0}\end{array}\right]\right]$$

Further expanding this gives:

$$S_{C1}(t) = L^{-1}\left[\frac{L}{\eta}\left[\begin{array}{l}(\rho_3+\mu)r_0+\rho_1 v_{P0}+\rho_1 n\Lambda t^2+\rho_2 v_{S0}-\nu_3 s_{C0}\\ -K\beta(q_1 e_0+q_2 i_0+q_3 b_0)s_{C0}\end{array}\right]\right]$$

Now, we can express $S_{C1}(t)$ in terms of the Laplace inverse, leading to:

$$S_{C1}(t) = L^{-1}\left[\frac{(\rho_3+\mu)r_0+\rho_1 v_{P0}+\rho_2 v_{S0}-\nu_3 s_{C0}}{\eta^2}-\frac{K\beta(q_1 e_0+q_2 i_0+q_3 b_0)s_{C0}}{\eta^4}+\frac{\rho_1 n\Lambda}{\eta^5}\right]$$

This leads us to:

$$S_{C1}(t) = \left[(\rho_3+\mu)r_0+\rho_1 v_{P0}+\rho_2 v_{S0}-\nu_3 s_{C0}\right]t-\left[K\beta(q_1 e_0+q_2 i_0+q_3 b_0)s_{C0}\right]t^3+\left[\rho_1 n\Lambda t^4\right] \tag{37}$$

From the third equation in (37), we have:

$$\frac{dV_P}{dt} = n\Lambda+\nu_1 S_P-(\nu_2+\rho_1+\mu)V_P$$

Taking the Laplace transform results in:

$$L\left[\frac{dV_P}{dt}\right] = L\left[n\Lambda+\nu_1 S_P-(\nu_2+\rho_1+\mu)V_P\right] \tag{38}$$

Applying the property of the Laplace transform to the left side gives:

$$\eta L\left[\frac{dV_P}{dt}\right]-V_P(0) = L\left[n\Lambda+\nu_1 S_P-(\nu_2+\rho_1+\mu)V_P\right]$$

Rearranging yields:

$$L\left[\frac{dV_P}{dt}\right] = \frac{V_P(0)}{\eta}+\frac{L}{\eta}\left[n\Lambda+\nu_1 S_P-(\nu_2+\rho_1+\mu)V_P\right]$$

Taking the inverse Laplace transform, we have:

$$L^{-1}\left\{L\left[\frac{dV_P}{dt}\right]\right\} = L^{-1}\left[\frac{V_P(0)}{\eta}+L\frac{n\Lambda}{\eta}\right]+L^{-1}\left\{\frac{L}{\eta}\left[\nu_1 S_P-(\nu_2+\rho_1+\mu)V_P\right]\right\} \tag{39}$$

Since $V_P(0) = v_{P0}$, we find:

$$V_P(t) = L^{-1}\left[\frac{v_{P0}}{\eta}+L\frac{n\Lambda}{\eta}\right]+L^{-1}\left\{\frac{L}{\eta}\left[\nu_1 S_P-(\nu_2+\rho_1+\mu)V_P\right]\right\} \tag{40}$$

Continuing, we express $V_P(t)$ as:

$$V_P(t) = L^{-1}\left[\frac{v_{P0}}{\eta}+\frac{n\Lambda}{\eta^3}\right]+L^{-1}\left\{\frac{L}{\eta}\left[\nu_1 S_P-(\nu_2+\rho_1+\mu)V_P\right]\right\}$$

Further simplifying, we have:

$$V_P(t) = v_{P0}+n\Lambda t^2+L^{-1}\left\{\frac{L}{\eta}\left[\nu_1 S_P-(\nu_2+\rho_1+\mu)V_P\right]\right\}$$

Next, we apply the Adomian Decomposition method:

$$V_P(t) = V_{P0}(t)+V_{P1}(t)+V_{P2}(t)+\cdots+V_{Pn}(t) = \sum_{n=0}^{\infty}V_{Pn}(t) \tag{41}$$

Using the recombination formula, we get:

$$\sum_{n=0}^{\infty}V_{Pn}(t) = v_{P0}+n\Lambda t^2+L^{-1}\left\{\frac{L}{\eta}\left[\nu_1\sum_{n=0}^{\infty}S_{Pn}(t)-(\nu_2+\rho_1+\mu)\sum_{n=0}^{\infty}V_{Pn}(t)\right]\right\} \tag{42}$$

Initial Approximation

$$V_{P0}(t) = v_{P0} + n\Lambda t^2, \quad S_{P0}(t) = s_{P0} + (1-n)\Lambda t^2$$

First Iteration when $n = 0$

$$\sum_{n=0}^{\infty} V_{P_{n+1}}(t) = L^{-1}\left\{\frac{L}{\eta}\left[\nu_1 \sum_{n=0}^{\infty} S_{P0}(t) - (\nu_2+\rho_1+\mu)\sum_{n=0}^{\infty} V_{P0}(t)\right]\right\} \tag{43}$$

$$V_{P1}(t) = L^{-1}\left\{\frac{L}{\eta}\left[\nu_1\left(s_{P0} + (1-n)\Lambda t^2\right) - (\nu_2+\rho_1+\mu)\left(v_{P0} + n\Lambda t^2\right)\right]\right\}$$

$$V_{P1}(t) = L^{-1}\left\{\frac{L}{\eta}\left[\nu_1 s_{P0} + \nu_1(1-n)\Lambda t^2 - (\nu_2+\rho_1+\mu)v_{P0} - (\nu_2+\rho_1+\mu)n\Lambda t^2\right]\right\} \tag{44}$$

$$V_{P1}(t) = L^{-1}\left\{\frac{L}{\eta}\left[\nu_1 s_{P0} + \nu_1(1-n)\Lambda t^2 - (\nu_2+\rho_1+\mu)v_{P0} - (\nu_2+\rho_1+\mu)n\Lambda t^2\right]\right\} \tag{45}$$

$$V_{P1}(t) = L^{-1}\left\{\left[\frac{\nu_1 s_{P0}}{\eta^2} - \frac{(\nu_2+\rho_1+\mu)v_{P0}}{\eta^2} + \frac{\nu_1(1-n)\Lambda}{\eta^4} - \frac{(\nu_2+\rho_1+\mu)n\Lambda}{\eta^5}\right]\right\}$$

$$V_{P1}(t) = \left\{\left[(\nu_1 s_{P0} - (\nu_2+\rho_1+\mu)v_{P0})\,t + \nu_1(1-n)\Lambda t^3 - (\nu_2+\rho_1+\mu)n\Lambda t^4\right]\right\} \tag{46}$$

From the fourth variable, in (37) we also have

$$\frac{dV_S}{dt} = \nu_2 V_P - (\mu+m)V_S - \rho_2 V_S + \nu_3 S_C \tag{47}$$

Taking the Laplace transform:

$$L\left[\frac{dV_S}{dt}\right] = L\left[\nu_2 V_P - (\mu+m)V_S - \rho_2 V_S + \nu_3 S_C\right]$$

$$\eta L\left[\frac{dV_S}{dt}\right] - V_S(0) = L\left[\nu_2 V_P - (\mu+m)V_S - \rho_2 V_S + \nu_3 S_C\right]$$

$$L\left[\frac{dV_S}{dt}\right] = \frac{V_S(0)}{\eta} + \frac{L}{\eta}\left[\nu_2 V_P - (\mu+m)V_S - \rho_2 V_S + \nu_3 S_C\right]$$

Since $V_S(0) = v_{S0}$:

$$L\left[\frac{dV_S}{dt}\right] = \frac{v_{S0}}{\eta} + \frac{L}{\eta}\left[\nu_2 V_P - (\mu+m)V_S - \rho_2 V_S + \nu_3 S_C\right]$$

Taking Laplace inverse:

$$L^{-1}\left\{L\left[\frac{dV_S}{dt}\right]\right\} = L^{-1}\left[\frac{v_{S0}}{\eta}\right] + L^{-1}\left\{\frac{L}{\eta}\left[\nu_2 V_P - (\mu+m)V_S - \rho_2 V_S + \nu_3 S_C\right]\right\} \tag{48}$$

$$V_S(t) = v_{S0} + L^{-1}\left\{\frac{L}{\eta}\left[\nu_2 V_P - (\mu+m)V_S - \rho_2 V_S + \nu_3 S_C\right]\right\}$$

Then Adomian Decomposition:

$$V_S(t) = V_{S0}(t) + V_{S1}(t) + V_{S2}(t) + \ldots + V_{Sn}(t) = \sum_{n=0}^{\infty} V_{Sn}(t) \tag{49}$$

$$\sum_{n=0}^{\infty} V_{Sn}(t) = v_{S0} + L^{-1}\left\{\frac{L}{\eta}\left[\nu_2 V_P - (\mu+m)V_S - \rho_2 V_S + \nu_3 S_C\right]\right\}$$

Initial Approximation:

$$V_{Sn}(t) = v_{S0}, \quad V_{P0}(t) = v_{P0} + n\Lambda t^2, \quad S_{C0}(t) = s_{C0}$$

First Iteration, when $n = 0$:

$$\sum_{n=0}^{\infty} V_{S_{n+1}}(t) = L^{-1}\left\{\frac{L}{\eta}\left[\nu_2 \sum_{n=0}^{\infty} V_{P0}(t) - (\mu+m)\sum_{n=0}^{\infty} V_{S0}(t) - \rho_2 \sum_{n=0}^{\infty} V_{S0}(t) + \nu_3 \sum_{n=0}^{\infty} S_{C0}(t)\right]\right\} \tag{50}$$

$$V_{S1}(t) = L^{-1}\left\{\frac{L}{\eta}\left[\nu_2(v_{P0} + n\Lambda t^2) - (\mu+m)v_{S0} - \rho_2 v_{S0} + \nu_3 s_{C0}\right]\right\}$$

$$V_{S1}(t) = L^{-1}\left\{\frac{L}{\eta}\left[\nu_2 v_{P0} - (\mu + m + \rho_2)v_{S0} + \nu_3 s_{C0} + \nu_2 n\Lambda t^2\right]\right\}$$

$$V_{S1}(t) = L^{-1}\left\{\frac{(\nu_2 v_{P0} - (\mu + m + \rho_2)v_{S0} + \nu_3 s_{C0})}{\eta^2} + \frac{\nu_2 n\Lambda}{\eta^4}\right\}$$

$$V_{S1}(t) = (\nu_2 v_{P0} - (\mu + m + \rho_2)v_{S0} + \nu_3 s_{C0})t + \nu_2 n\Lambda t^3 \tag{51}$$

Also from fifth equation of (37)

$$\frac{dE}{dt} = \beta(q_1 E + q_2 I + q_3 B)(S_P + K S_C - (\mu + z)E$$

Taking the Laplace transform

$$L\left[\frac{dE}{dt}\right] = L\left[\beta(q_1 E + q_2 I + q_3 B)(S_P + K S_C - (\mu + z)E\right] \tag{52}$$

$$\eta L\left[\frac{dE}{dt}\right] - E(0) = L\left[\beta(q_1 E + q_2 I + q_3 B)(S_P + K S_C - (\mu + z)E\right]$$

$$L\left[\frac{dE}{dt}\right] = \frac{E(0)}{\eta} + \frac{L}{\eta}\left[\beta(q_1 E + q_2 I + q_3 B)(S_P + K S_C - (\mu + z)E\right]$$

Since E(0)=e_0

$$L\left[\frac{dE}{dt}\right] = \frac{e_0}{\eta} + \frac{L}{\eta}\left[\beta(q_1 E + q_2 I + q_3 B)(S_P + K S_C - (\mu + z)E\right]$$

Taking Laplace inverse

$$L^{-1}\left\{L\left[\frac{dE}{dt}\right]\right\} = L^{-1}\left[\frac{e_0}{\eta}\right] + L^{-1}\left\{\frac{L}{\eta}\left[\beta(q_1 E + q_2 I + q_3 B)(S_P + K S_C - (\mu + z)E\right]\right\}$$

$$E(t) = e_0 + L^{-1}\left\{\frac{L}{\eta}\left[\beta(q_1 E + q_2 I + q_3 B)(S_P + K S_C - (\mu + z)E\right]\right\}$$

Adomia decomposition

$$E(t) = E_0(t) + E_1(t) + E_2(t) + ...E_n(t) = \sum_{n=0}^{\infty} E_n(t)$$

Recommence Formula

$$\sum_{n=0}^{\infty} E_n(t) = e_0 + L^{-1}\left\{\frac{L}{\eta}\left[\beta(q_1 E + q_2 I + q_3 B)(S_P + K S_C - (\mu + z)E\right]\right\}$$

$$\sum_{n=0}^{\infty} E_{n+1}(t) = e_0 + L^{-1}\left\{\frac{L}{\eta}\left[\begin{array}{l}\beta(q_1 \sum_{n=0}^{\infty} E_0(t) + q_2 \sum_{n=0}^{\infty} I_0(t) + q_3 \sum_{n=0}^{\infty} B_0(t))(\sum_{n=0}^{\infty} S_{P0}(t) \\ +K \sum_{n=0}^{\infty} S_{C0}(t) - (\mu + z) \sum_{n=0}^{\infty} E_0(t)\end{array}\right]\right\}$$

Initial Approximation

$$E_0(t) = e_0,\ I_0(t) = i_0,\ B_0(t) = b_0,\ S_{P0}(t) = s_{P0} + (1 - n)\Lambda t^2,\ S_{C0}(t) = s_{c0}$$

First iteration when n=0

$$E_1(t) = L^{-1}\left\{\frac{L}{\eta}\left[\begin{array}{l}\beta(q_1 e_0 + q_2 i_0 + q_3 b_0)(s_{P0} + (1 - n)\Lambda t^2 \\ +K s_{C0}) - (\mu + z)e_0\end{array}\right]\right\}$$

$$E_1(t) = L^{-1}\left\{\frac{L}{\eta}\left[\begin{array}{l}\beta(q_1 e_0 + q_2 i_0 + q_3 b_0)s_{P0} + \beta(q_1 e_0 + q_2 i_0 + q_3 b_0)(1 - n)\Lambda t^2 \\ +\beta(q_1 e_0 + q_2 i_0 + q_3 b_0)K s_{C0}) - (\mu + z)e_0\end{array}\right]\right\}$$

$$E_1(t) = L^{-1}\left\{\left[\begin{array}{l}\frac{\beta(q_1 e_0 + q_2 i_0 + q_3 b_0)s_{P0}}{\eta^3} + \frac{\beta(q_1 e_0 + q_2 i_0 + q_3 b_0)(1 - n)\Lambda}{\eta^5} \\ +\frac{\beta(q_1 e_0 + q_2 i_0 + q_3 b_0)K s_{C0})}{\eta^4} - \frac{(\mu + z)e_0}{\eta^2}\end{array}\right]\right\}$$

$$E_1(t) = \left\{\left[\begin{array}{l}-(\mu + z)e_0 t + \beta(q_1 e_0 + q_2 i_0 + q_3 b_0)s_{P0} t^2 + \beta(q_1 e_0 + q_2 i_0 + q_3 b_0)K s_{C0})t^3 \\ \beta(q_1 e_0 + q_2 i_0 + q_3 b_0)(1 - n)\Lambda t^4\end{array}\right]\right\}$$

And the first two approximate model result yields:

$$S_P(t) = \sum_{n=0}^{2} S_{P,0,n}, \qquad V_P(t) = \sum_{n=0}^{2} V_{P,0,n}, \qquad S_C(t) = \sum_{n=0}^{2} S_{C,0,n},$$
$$E(t) = \sum_{n=0}^{2} E_{0,n}, \qquad I(t) = \sum_{n=0}^{2} I_{0,n}, \qquad Q(t) = \sum_{n=0}^{2} Q_{0,n},$$
$$R(t) = \sum_{n=0}^{2} R_{0,n}, \qquad B(t) = \sum_{n=0}^{2} B_{0,n}.$$

3.8. Convergence Analysis

In this section, we refer to [14] to demonstrate the convergence of the solution. The iterative solution (3.7) can be illustrated as

$$\nu_n = \Omega\nu_{n-1}, \quad \nu_{n-1} = \sum_{j=1}^{n} \nu_j, \quad n = 1, 2, 3, \ldots \tag{53}$$

and we prove the convergence of $\{\nu_n\}$ using the subsequent theorem.

Theorem 2 *Let B_1 be a Banach Space and $\Omega : B_1 \to B_1$ a contraction mapping with constant $0 < \delta < 1$. Then, there exists a unique point υ in Ω such that $\Omega(\upsilon) = \upsilon$ and $\upsilon = (S, V, P, I, H, R, B)$. Let $\upsilon_0 \in P_s(\upsilon)$, where $P_s(\upsilon) = \{\upsilon' \in B_1 : \|\upsilon' - \upsilon\| < s\}$. Then, we have $\upsilon_m \in P_s(\upsilon)\, \forall m$ and $\upsilon_m \to \upsilon$.*

Proof
Using mathematical induction, when $m = 1$, we have

$$\|\upsilon_0 - \upsilon\| = \|\Omega(\upsilon_0) - \Omega(\upsilon)\| \leq \delta\|\upsilon_0 - \upsilon\|.$$

Assuming the statement is true for m, we have

$$\|\upsilon_{m-1} - \upsilon\| \leq \delta^{m-1}\|\upsilon_0 - \upsilon\|.$$

Thus,

$$\|\upsilon_n - \upsilon\| = \|\Omega(\upsilon_{n-1}) - \Omega(\upsilon)\| \leq \delta\|\upsilon_{m-1} - \upsilon\| \leq \delta^m\|\upsilon_0 - \upsilon\|.$$

Again, since $\upsilon_0 \in P_s(\upsilon)$, we have $\|\upsilon_0 - \upsilon\| < s$ and

$$\|\upsilon_n - \upsilon\| \leq \delta^m\|\upsilon_0 - \upsilon\| < \delta^m s < s.$$

Consequently, this proves that $\upsilon_m \in P_s(\upsilon)$. Moreover, since

$$\lim_{m\to\infty} \delta^m = 0,$$

therefore,

$$\lim_{m\to\infty} \delta^m\|\upsilon_n - \upsilon\| = 0,$$

and

$$\lim_{m\to\infty} \upsilon_m = \upsilon,$$

which completes the proof. Comparatively, numerical iteration of Laplace Adomian Decomposition method with the Homotopy perturbation method for the model solution as the forthcoming sections will delve into the analysis of the homotopy perturbation method, elucidating its application and implications in our quest for a solution.

$$\Delta(\alpha) = \kappa(\tau) \quad \tau \in \lambda \tag{54}$$

Subject to the boundary condition

$$\Psi(\alpha, \alpha_n) = 0 \quad \tau \in \prod \tag{55}$$

Operator Δ represents the differential operator, Ψ denotes the boundary operator, $\kappa(\tau)$ is an analytic function, Φ is a defined domain bounded by $\prod$, and $\alpha_n$is a normal vector derivative drawn externally from Φ. Thus we can separate the operator $\Delta(\alpha)$ into two:

$$\Delta(\alpha) = L_T(\alpha) + N_T(\alpha) \tag{56}$$

The operator $L_{T(\alpha)}, N_{T(\alpha)}$ denotes the linear and nonlinear term respectively such that equation implies:

$$L_T(\alpha) + N_T(\alpha) = \kappa(\tau) \quad \tau \in \lambda \tag{57}$$

We can construct a Homotopy so that

$$H(f,p) = (1-p)[L_T(f) - L_T(\omega_0)] + p[\Delta(f) - \kappa(\tau)] = 0 \tag{58}$$

Where p is an embedding parameter which can undergo a deformation process of changing from $[0,1]$. Equation the below equation is further simplified to obtain:

$$H(f,p) = L_T(f) - L_T(\alpha_0) + p[L_T(\alpha_0)] + p[N_T(\alpha_0) - \kappa(\tau)] = 0 \tag{59}$$

as equation $p \to 1$ yields:

$$H(f,0) = L_T(f) - L_T(\alpha_0) = 0 \tag{60}$$

And when $p \to 1$ yields:

$$H(f,1) = \Delta(f) - \kappa(\tau) = 0 \tag{61}$$

We can naturally assume the solution as a power series such that

$$f(t) = f_0(t) + pf_1(t) + p^2 f_2(t) + \cdot^n f_n(t) \tag{62}$$

Evaluating the above equations, and comparing coefficients of equal powers of p.The values of $f_0(t), f_1(t), f_2(t)$ are obtained by solving the resulting ordinary differential equations. Thus, the approximate solution is obtained as:

$$f(t) = \lim_{p\to 1} f_n(t) = f_1(t) + f_2(t) + f_3(t) + \cdot \tag{63}$$

To conduct numerical simulation on the mathematical model, we create the following iterative for the model equation.

$$\begin{aligned}
&(1-p)\frac{dS_P}{dt} + p\left((1-n)\Lambda - \beta(q_1E + q_2I + q_3B) - (V_1+\mu)S_P\right),\\
&(1-p)\frac{dV_P}{dt} + p\left(n\Lambda + V_1S_P - (v_2+p_1+\mu)V_P\right),\\
&(1-p)\frac{dS_C}{dt} + p\left((\rho_3+\mu)R + \rho_1V_P + \rho_2V_S - V_3S_C - K\beta(q_1E + q_2I + q_3B)S_C\right),\\
&(1-p)\frac{dV_S}{dt} + p\left(v_2V_P - (\mu+m)V_S - \rho_2V_S + V_3S_C\right),\\
&(1-p)\frac{dE}{dt} + p\left(\beta((q_1E + q_2I + q_3B)(S + KS_C) - (\mu+Z)E)\right),\\
&(1-p)\frac{dI}{dt} + p\left(ZE - (\Upsilon_1 + \Upsilon_2 + \mu + \delta_1 + \mu)I\right),\\
&(1-p)\frac{dQ}{dt} + p\left(\Upsilon_1 I - (\tau + \Upsilon_3 + \delta_2 + \mu)Q\right),\\
&(1-p)\frac{dR}{dt} + p\left(\Upsilon_2 I + (\tau+\Upsilon_3)Q + mV_S - (\mu+\rho_3)R\right),\\
&(1-p)\frac{dB}{dt} + p\left(\omega + \xi_1E + \xi_2I - \mu_bB\right).
\end{aligned} \tag{64}$$

Simplifying the preceding equation above results in the respective iterations.The results obtained are similar to that of (LADM), but in comparison of convergence, LADM gives more accurate and desired result to the research study.

4. Results

In this section, numerical simulations were performed on the mathematical model to evaluate the transmission dynamics of cholera within the human population and the results are presented as graphs. The simulations were carried out using the Maple 18 software.

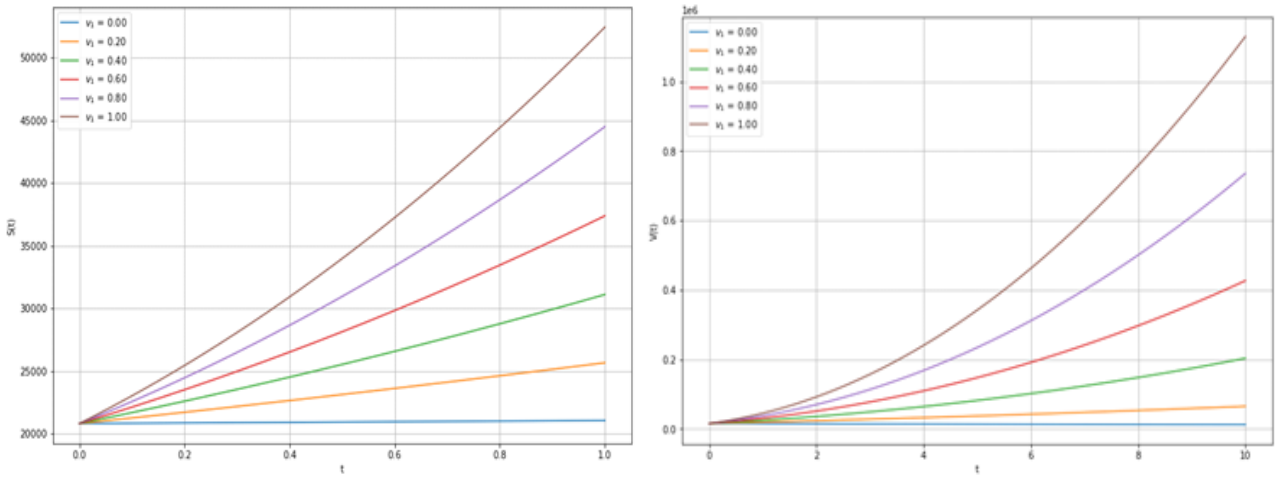

(A) (B)

Figure 2. The Impact of Childhood Immunization on Cholera Eradication

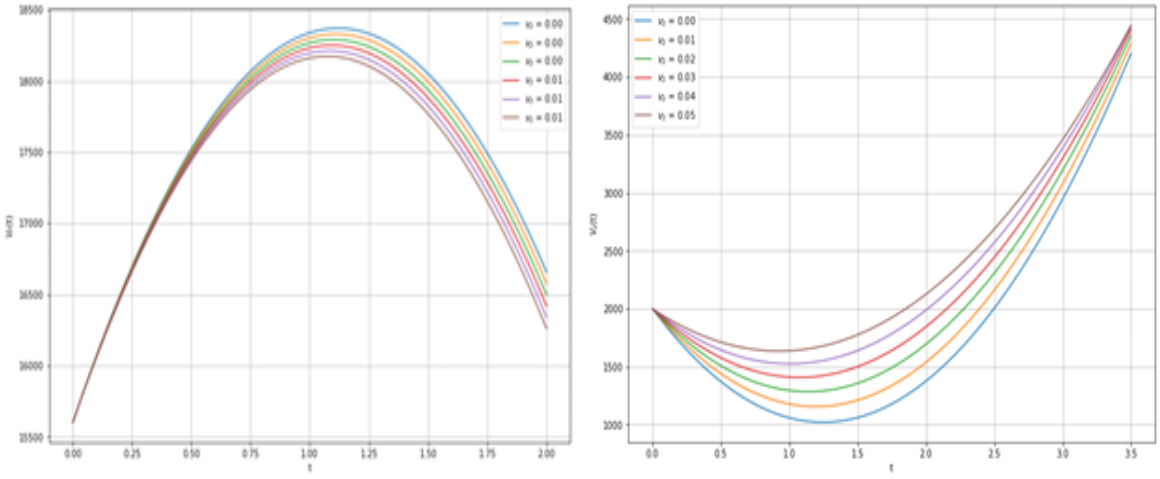

(A) (B)

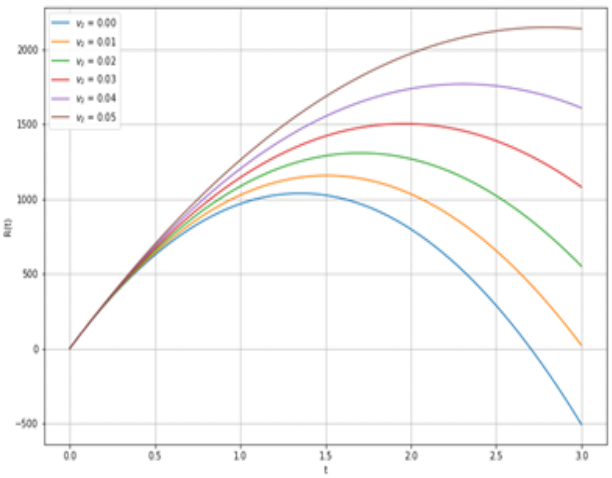

(C)

Figure 3. The Effect of Imperfect Adult Vaccination on Susceptible and Partially Immune Populations

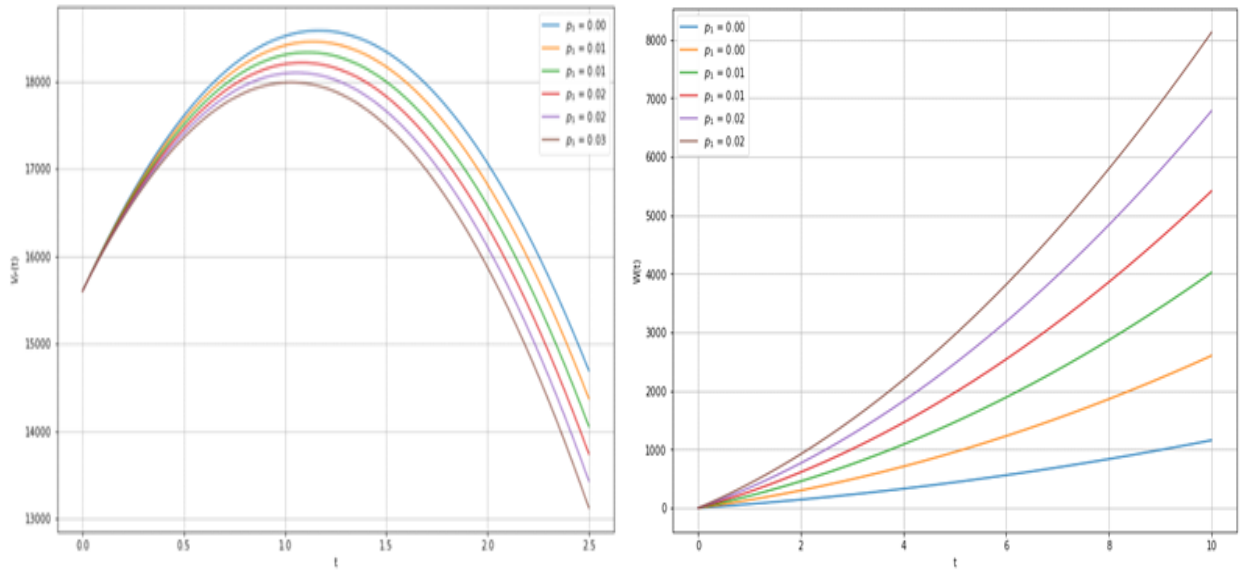

(A) (B)

Figure 4. The Effect of a Perfect Vaccine Dose on Partially Immune, Boosted, and Recovered Populations

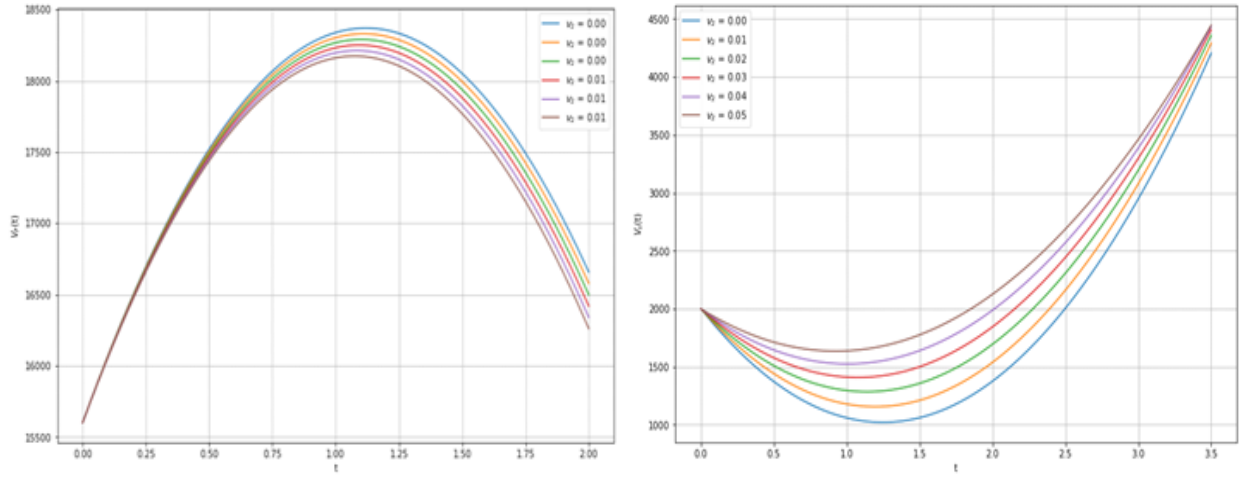

(A) (B)

Figure 5. The Effect of Waning Immunity Due to Imperfect Vaccination

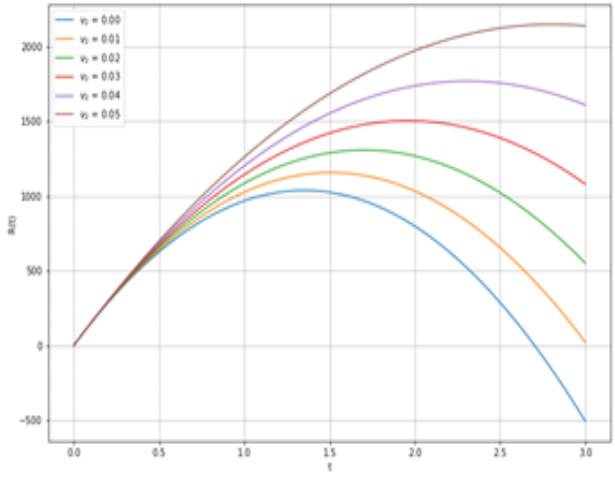

Figure 6. The Effect of Waning Immunity Due to Immunosenescence of Secondary Vaccine

5. Discussion

The results of the numerical simulations provide critical insights into the impact of vaccination on cholera dynamics within human populations. Figure 1A illustrates how childhood immunization significantly reduces susceptibility to cholera over time, with a notable decline in vulnerability observed eight years after the initiation of infant vaccination programs. This graph underscores the pivotal role of early immunization in decreasing individual risk and enhancing community resilience against cholera outbreaks. In Figure 1B, the focus shifts to the impact of increased primary vaccination coverage among infants. The rising curve demonstrates a corresponding enhancement in population-level immunity, highlighting the effectiveness of widespread vaccination initiatives in bolstering community defenses against cholera. This graph emphasizes the importance of high vaccination coverage rates among infants to achieve herd immunity and curb disease transmission. Figure 1C delves into the controlled growth of cholera-exposed individuals post-vaccination. The graph illustrates a managed increase in the number of exposed individuals, underscoring the efficacy of targeted immunization strategies in limiting the spread of cholera within vaccinated populations. This figure highlights how focused vaccination efforts can mitigate the impact of outbreaks by reducing the pool of susceptible individuals. Figure 2A reveals heightened susceptibility to cholera in regions where adult vaccination coverage remains inadequate. This stark depiction underscores the vulnerabilities that persist when vaccination efforts do not reach all segments of the population, emphasizing the need for comprehensive immunization strategies across all age groups to achieve robust protection. Complementing this, Figure 2B illustrates a rise in partially immune individuals despite adult vaccination efforts. This graph stresses the importance of closing immunity gaps through comprehensive coverage, as partial immunity can still contribute to disease transmission and outbreak dynamics. Figure 3A correlates secondary doses with enhanced immunity, illustrating how additional vaccine doses strengthen protection against cholera over time. Figure 3B depicts the increasing proportion of individuals achieving perfect immunity through vaccination, demonstrating the cumulative effect of effective vaccination strategies in building population resilience. Furthermore, Figure 3C underscores the benefits of vaccination by showing a rising trend in recovery rates post-vaccination, emphasizing the broader public health benefits of vaccination programs in reducing disease severity and accelerating recovery times among affected individuals. Figure 4A notes the declining numbers of individuals protected by primary vaccination due to waning immunity over time. This highlights the challenge of maintaining long-term protection against cholera without supplementary measures such as booster doses. Figure 4B addresses the rapid waning of immunity post-vaccination, emphasizing the need for robust booster strategies to sustain protective immunity levels among vaccinated populations. This figure advocates for proactive approaches to maintaining vaccine effectiveness and preventing the resurgence of cholera outbreaks. Finally, Figure 5 emphasizes the declining immunity among previously recovered individuals, reinforcing the necessity of sustained vaccination efforts through additional boosters to maintain community-wide protection. Collectively, these insights underscore the imperative nature of comprehensive vaccination strategies in mitigating cholera and ensuring enduring public health resilience against infectious diseases.

6. Limitation to study

A limitation of this study is that the mathematical model, while incorporating key epidemiological factors and intervention strategies such as booster vaccination and quarantine, relies on several simplifying assumptions that may not fully capture the complexities of real-world on cholera dynamics. The model assumes homogeneous mixing of the population and constant parameter values over time, which may not reflect variations in human behaviour, environmental factors, access to healthcare or regional disparities in infrastructure. Additionally, the model does not account for potential logistical challenges in implementing vaccination and quarantine measures, such as vaccine availability, public compliance, identification and isolation of infected individuals. These factors could significantly influence the effectiveness of the proposed interventions in actual outbreak scenarios.

7. Conclusion

In conclusion, our study demonstrates that booster vaccination and effective quarantine measures are critical interventions for controlling cholera. The findings indicate that targeted booster campaigns significantly enhance population immunity and reduce cholera incidence, particularly during outbreaks. Additionally, well-implemented quarantine protocols play a vital role in curbing the disease's spread by isolating infected individuals swiftly. The integration of these strategies offers a robust approach to cholera control, leading to greater reductions in incidence compared to singular interventions. Implementing these recommendations can strengthen cholera control efforts and improve public health outcomes.

Acknowledgments

Authors would like to express their gratitude to the anonymous reviewers that improved this manuscript.

References

1. S. Adebayo and M. Kolawole. Mathematical modeling and analysis of cholera control strategies in resource-limited regions. *Uniosun Journal of Engineering and Environmental Sciences*, 7(1):249–262, 2025.
2. J. Adedeji and M. Olayiwola. On analysis of a mathematical model of cholera using Caputo fractional order. *Journal of the Nigerian Mathematical Society*, 43(3):287–309, 2024.
3. N. Ahmaed G, Hasan. Colony blot hybridization method for enumeration of culturable vibrio cholerae and vibrio mimicus bacteria. *Applied and Environmental Microbiology*, 75(17):54–79, 2023.
4. S. Aydogn and H. Mohammadi. On modeling of epidemic childhood diseases with the Caputo-Fabrizio derivative by using the Laplace Adomian decomposition method. *Alexandria Engineering Journal*, 5(59):30–59, 2024.
5. T. Ayoola, A. Popoola, M. Olayiwola, and A. Alaje. Mathematical modeling of chickenpox transmission using the Laplace adomian decomposition method. *Results in Control and Optimization*, 9(4):85105, 2024.
6. T. Das-Eeur and K. Angelis. The impact of Measles-Rubella vaccination on the morbidity and mortality from Congenital Rubella syndrome in 92 countries. *Biological Theory and Methods*, 2(15):309316, 2021.
7. Z. Dere and G. Sobamowo. Analytical solutions of black-scholes partial differential equation of pricing for valuations of financial options using hybrid transformation methods. *The Journal of Engineering and Exact Sciences*, 8(1):152, 2024.
8. W. Dressler. Modernization, stress, and blood pressure: New directions in research. *International Journal of Epidemiology,*, 4(71):583605, 2023.
9. S. Edward and N. Nkuba. Modeling analysis and numerical solution to malaria fractional model with temporary immunity and relapse. *Tanzania Journal of Sciences*, 4(2):5363, 2024.
10. S. Faruque and Naser. Hydroclimatic influences on seasonal and spatial cholera transmission cycles: Implications for public health intervention in the bengal delta. *The Indonesian Juornal of Public Health*, 10(5):115129, 2023.
11. P. J. Grant and S. D. Anker. Guidelines on diabetes, pre-diabetes, and cardiovascular diseases developed in collaboration with the EASD. *European Heart Journal*, 3(39):29–42, 2023.
12. M. Harris and C. Thomas. Molecular and epidemiological characterization of toxigenic and non toxigenic corynebacterium diphtheriae, corynebacterium belfantii, corynebacterium rouxii, and corynebacterium ulcerans isolates identified in spain from 2014 to 2019. *Journal of Clinical Microbiology*, 59(4):59–72, 2022.
13. M. Kolawole and B. Akin-awoniran. On the numerical analysis of the effect of vaccine on measles using virational iteration method. *Jurnal Diferensial*, 2(23):54–67, 2024.
14. M. Kolawole and R. Ayoola. A novel mathematical model evaluating the impact of saturated treatment response, vaccination and anti-biotic resistance on transmission dynamics of typhoid fever. *Uniosun Journal of Engineering and Environmental Sciences*, 7(1):264–280, 2025.
15. M. Kolawole and M. Olayiwola. Conceptual analysis of the combined effects of vaccination, therapeutic actions, and human subjection to physical constraint in reducing the prevalence of COVID-19 using the homotopy perturbation method. *Beni-Suef University Journal of Basic and Applied Sciences*, 2(18):2–20, 2023.
16. P. Kumar, R. Gupta, and S. Roy. Analysis of vaccination and quarantine strategies in cholera: A simulation study. *Computers and Mathematics with Applications*, 2(95):274–287, 2023.
17. N. M. and K. Davis. Evaluation of household water treatment technologies for cholera eradication in Sub-Saharan Africa. *Epidemiological and Mathematical Perspectives. Sustain*, 16(29):1–29, 2024.
18. K. Odeyemi and M. Kolawole. Stability analysis of (SVEITR) model for cholera control with treatment and vaccination using Laplace adomian decomposition method. *Jurnal Diferensial*, 7(1):85105, 2025.
19. N. K. Opoku and C. Afriyie. The role of control measures and the environment in the transmission dynamics of cholera. *Abstract in Mathematics and Applied Analysis*, 6(8):20–38, 2020.
20. T. Weng and S. Lee. Conflict and households acute food insecurity: evidences from the ongoing war in Tigrai-Northern Ethiopia. *Annals of Internal Medicine*, 3(14):18–44, 2024.
21. Z. Williams. Damage to the public health system caused by war-related looting or vandalism in the Tigray region of Northern Ethiopia. *Bulletin of Mathematical Biology*, 3(14):267–280, 2024.

